Available online at www.sciencedirect.com

ScienceDirect

Procedia Engineering 10 (2011) 189–194

Engineering Procedia

ICM11

The deformation and damage mechanisms during thermomechanical fatigue (TMF) in IN792

Jan Kanesund[a], Johan Moverare[a,b] and Sten Johansson[a]

[a]*Division of Engineering Materials, Department of Management and Engineering, Linköping University, SE-581 83 Linköping, Sweden*
[b]*Siemens Industrial Turbomachinery AB, Materials Technology, SE-61283 Finspong, Sweden*

Elsevier use only: Received date here; revised date here; accepted date here

Abstract

The deformation and damage mechanisms arising during thermomechanical fatigue (TMF) of the polycrystalline superalloy IN792 have been investigated. The TMF cycles used in this study are in-phase (IP) and out-of-phase (OP). The minimum temperature used in all TMF-tests is 100°C while the maximum temperature is 750°C in the IP TMF-tests and 850° or 950°C in the OP TMF-tests. Most cracks have propagated transgranularly through the material and this holds for all temperatures used in this study. In all tests, the cracks have initiated and propagated in locations where deformation structures such as deformation bands have formed in the material. In the temperature interval 750°-850°C, twins are formed in both IP and OP TMF-tests and this behaviour is observed to be further enhanced close to a crack. Twins are to a significantly lesser extent observed for tests with a higher (950°C) maximum temperature. Recrystallization at grain boundaries, around particles and within the deformation structures have occurred in the OP TMF-tests with a maximum temperature of 850° and 950°C and this is more apparent for the higher temperature.

Keywords: *nickel based superalloys, fatigue, deformation bands, recrystallization, twinning*

1. Introduction

The nickel-base superalloy IN792 is a cast polycrystalline material with high strength and excellent hot corrosion resistance [1-2]. Due to its good properties IN792 is widely used in hot sections in industrial and aircraft turbines and typical components used is turbine blades and vanes. An advantage of using nickel-based superalloy in this type of components is that it can withstand extreme levels of temperature and loading during many years of service before the component has reached its final life. The component can either be made as a single crystal or in polycrystalline form. However, polycrystalline material is more common due to lower cost and a simpler production route [3].

During service the critical turbine components are subjected to time dependent stress fields that originate from external forces and temperature gradients that are generated during engine start-up and shut-down. The gathering of such strain and temperature cycles can in the end lead to crack initiation phenomena often referred to as thermomechanical fatigue (TMF). Traditionally, the critical hot section components have been designed with respect to creep. However, today the deformation characteristics under TMF conditions are just as important and need to be understood if component lifetime estimates are to be accurate [4-5]. The TMF failure is promoted when plastic

Selection and peer-review under responsibility of ICM11 doi:10.1016/j.proeng.2011.04.034

strain cannot be accommodated at low temperatures and creep deformation together with oxidation occurs at high temperature. The stress/strain and temperature cycles can be completely independently of each other and the two most common cycles used for TMF testing are in-phase (IP) and out-of-phase (OP). In IP TMF-tests the material undergoes creep relaxation in tension at high temperature and plastic deformation in compression at low temperature. In OP TMF-tests, the material undergoes creep relaxation in compression at high temperature and plastic deformation in tension at low temperature.
The research reported in the present paper focus on the deformation and damage mechanisms in a cast polycrystalline nickel-base superalloy during TMF and the influence of both temperature range and cycle type have been investigated through a large number of carefully conducted TMF experiments followed by comprehensive microstructure characterizations using scanning electron microscopy.

2. Experimental procedure

All tests in this study were done on IN792, a γ'-precipitation hardened nickel-based superalloy. The chemical composition is Ni–12.4Cr–8.9Co–1.8Mo-4.0W-3.5Al–4.0Ti–4.1Ta–0.08C–0.017B-0.019Zr (wt-%). After conventional casting the material was hot isostatically pressed (HIP) at 1195°C and 150 MPa for 2 h followed by solution heat treatment at 1121ºC for 2 h and ageing at 850ºC for 24 h. Rotational symmetric test bars with a parallel length of 24 mm and a diameter of 6.0 mm were machined from the cast bars which had an initial diameter of 20 mm.
TMF tests can be performed with an arbitrary phase shift (φ) between the temperature and the mechanical loading. In this study, in-phase (φ=0°) and out-of-phase (φ=180°) tests have been considered. All tests were conducted using an MTS 810 servo-hydraulic thermomechanical fatigue machine where induction heating and forced air cooling is used in order to cycle the temperature. The minimum temperature in all tests was 100°C while the maximum temperature was either 750°C, 850°C or 950°C. Strain was measured by an axial extensometer and all tests were done in mechanical strain control (i.e. with a fixed total strain range compensated for thermal expansion $\Delta\varepsilon = \varepsilon_{max} - \varepsilon_{min}$). The strain ratios ($R = \varepsilon_{min} / \varepsilon_{max}$) where always $R = 0$ for the IP tests and $R = -\infty$ for the OP tests. Even if significant plastic deformation occur in the first cycle, sufficient creep relaxation during the hold time at the maximum temperature is typically necessary to establish a stabilized mean stress. Thus, in order to achieve a stabilized mean stress early in the tests, a 20 hour hold time was applied at the maximum temperature (T_{max}) during the first cycle. For all subsequent cycles a 5 minute hold time was applied. This combination of R-ratio and longer hold time in the first cycle was chosen since it better represents the real situation for most engineering components under OP-TMF or IP-TMF loading, see reference [5] for further details.
After the testing the ruptured fatigue specimens were sectioned parallel to the longitudinal axis for microstructural investigations. For comparison, also virgin (untested) material has been investigated. All samples were prepared by grinding and mechanical polishing. The samples are than analysed using scanning electron microscopy (SEM). In order to obtain optimal channelling contrast in the image, a backscatter electron detector on a Hitachi SU70 FEGSEM operating at 10 kV was used. The contrast in such an image is associated with discontinuities in the specimen and any crystallographic defect that produces a distortion in the lattice, such as a twin, a sub-grain or dislocation can be observed. Such images are similar in appearance to transmission electron micrographs, but with lower image resolution [6].
Orientation imaging microscopy (OIM) was performed using an electron back-scattering diffraction (EBSD) system from HKL Technology. By using EBSD analysis the actual presence of twins can be confirmed since they have a misorientation of 60° compared to the surrounding material. In case recrystallization has occurred new grains are formed with an arbitrary misorientation. In the OIM figures, grain orientations are represented by different colours and the grain boundaries are coloured black or grey depending of their misorientation. In order to obtain satisfying results from the EBSD analyses noise reduction has been carried out.

3. Experimental results

3.1. Virgin microstructure

In792 is a conventional cast polycrystalline nickel-based superalloy and the typically microstructure is rather coarse-grained and a lot of carbides and borides precipitate in grain boundaries and in the interdendritic regions see fig. 1a.

The microstructure consist of γ-phase, γ'-phase and γ/γ' eutecticum and the primary γ'-phase can have both a cubic and an irregular appearance and the size of them are about 0.6-0.7 µm see fig. 2b.

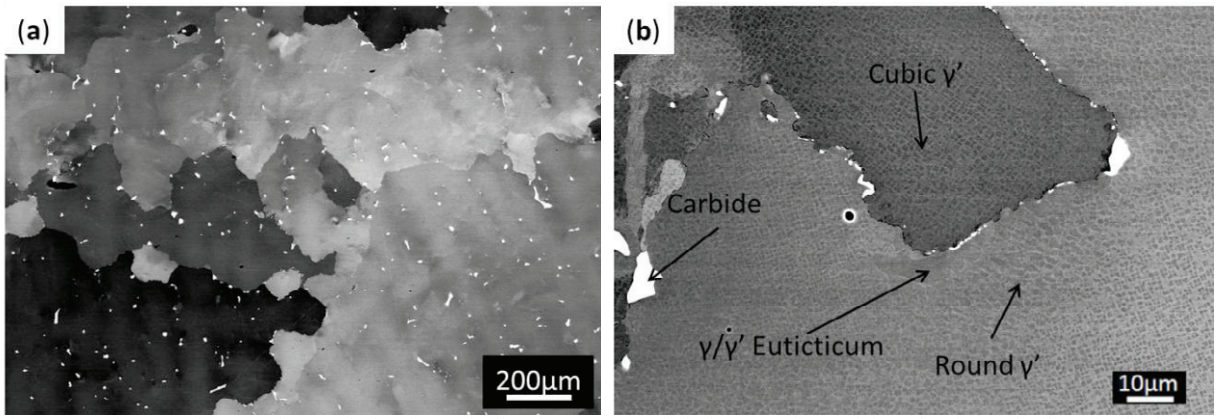

Figure 1: Backscatter electron micrograph showing typically microstructure of virgin untested material, a) showing typically grain size in the material, b) showing cubic and irregular appearance of γ'-phase and γ'/γ eutecticum.

3.2. IP TMF 100-750°C

Fig. 2 a-c show material which has been exposed to an IP TMF test where the temperature is cycled in the interval 100-750°C. The cracks have propagated transcrystalline in the material, in the zones where different types of deformation structures can be seen. In the same area multiple cracking and crack branching have occurred and some of the cracks have stopped propagating after a while, see fig. 2 a. At higher magnification, different types of dislocation structures and twins are seen in the deformation structure. Twins are found on the both sides of the crack and at the left hand side the twins are parallel to the crack, see fig. 2 b-c.

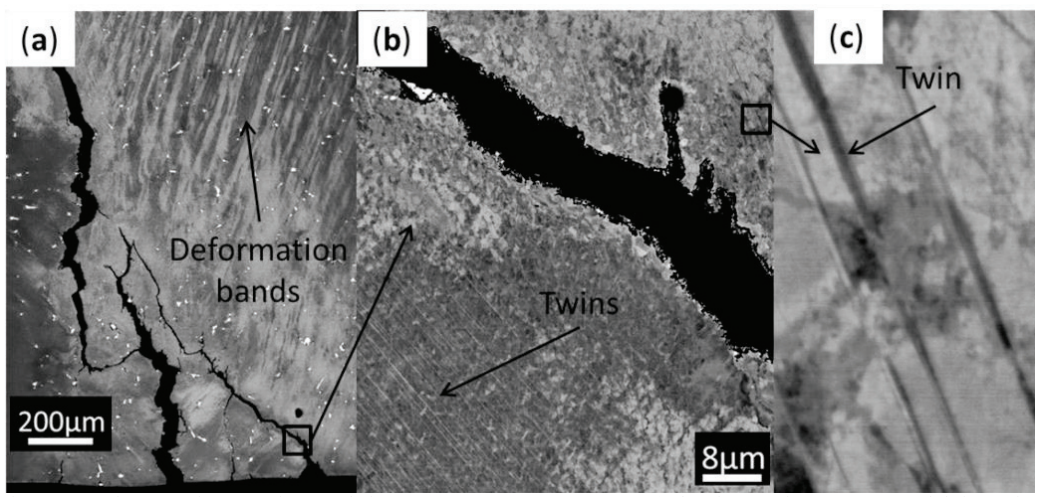

Figure 2: Backscatter electron micrograph from an IP TMF 100-750°C test, a) showing crack appearance and deformation structure, b) and c) showing dislocation structures and twins. Stress axis in horizontal direction.

3.3. OP TMF 100-850°C

Fig. 3a-b show material which has been exposed to an OP TMF test where the temperature is cycled in the interval 100-850°C. In fig. 3a, the crack has propagated transgranularly transverse to the applied load, in the zone where different types of deformation structures can be seen. At higher magnification, different types of dislocation structures and twins are observed in the deformation structure, see fig. 3b. Fig. 3c shows the results from an EBSD

analysis made in the same area where twins can be seen in fig. 3b. Fig. 3c shows both an orientation image map and a misorientation profile that confirm twinning due to the misorientation of 60° between the twins and surrounding material.

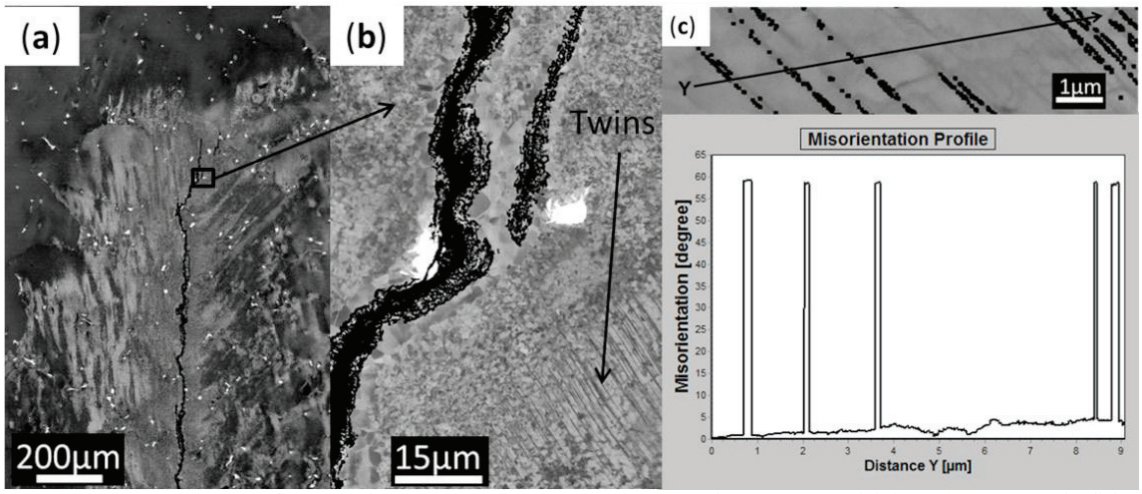

Figure 3: Backscatter electron micrograph from an OP TMF 100-850°C test, a) crack appearance and deformation structure, b) dislocation structures and twins, c) results from an EBSD analyze showing an orientation image map and a misorientation profile that confirm twinning. Stress axis in horizontal direction.

3.4. OP TMF 100-950°C

Fig. 4a-b and fig. 5a show material which is exposed to an OP TMF test where the temperature is cycled in the interval 100-950°C. Near the fracture surface different types of deformation structures have been formed, see fig 4a-b. Recrystallization has occurred in the deformation structures and in the grain boundaries, see fig. 4a. Fig. 5a shows that recrystallization has occurred at the grain boundaries since many small grains have been formed between the larger grains. Fig. 5b-c show the results from an EBSD analysis made in the same area as fig. 5a and the orientation image map and the misorientation profile confirm recrystallization.

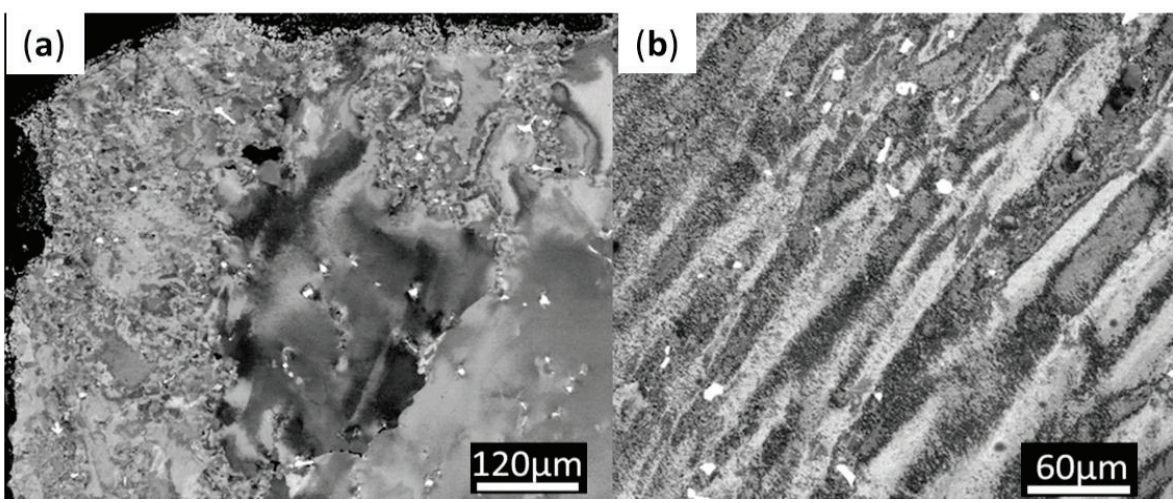

Figure 4: Backscatter electron micrograph from an OP TMF 100-950°C test showing the appearance near the fracture surface a) deformation structure with recrystallization , b) deformation structure consisting of deformation bands. Stress axis in horizontal direction.

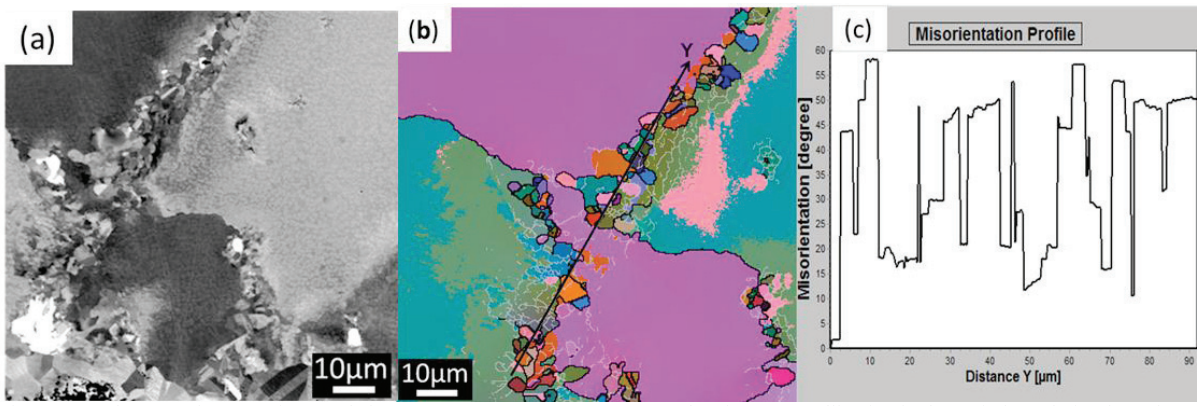

Figure 5: Backscatter electron micrograph from an OP TMF 100-950°C test, a) showing recrystallization in the grain boundaries, b) and c) EBSD orientation image map and misorientation profile (along the y-axis) confirming recrystallization at the grain boundaries. Stress axis in horizontal direction.

4. Discussion

The aim of the present study is to obtain a deeper understanding of the deformation and damage mechanisms active during thermomechanical fatigue (TMF). Most cracks have propagated transgranularly through the material and this holds for all temperatures used in this study. All cracks observed in this study have propagated in zones where the material is strongly plastically deformed. In these zones different types of deformation structures are formed and they consist of different types of deformation bands, as is shown in fig. 2a and 3a. The presence of deformation bands have been observed in fatigued copper single and bi-crystals by Zhang et al. and Li et al. [6,7]. Both of them have studied the deformation bands and observed that they consist of different dislocation structures, such as persistent slip bands, veins, dislocation walls and misorientation cell structure. Buque at al. [8] have made a study of dislocation structure in cyclically deformed pure nickel polycrystals and he observed that different dislocation structures such as fragmented wall, labyrinth, bundle, patch structure are formed in different crystallographic direction during cyclic deformation.

Another deformation mechanism which is frequently observed in this study of IN792 is twinning. Twins are observed in both IP and OP tests and they are most common for TMF cycles with maximum temperatures of 750° and 850°C, see fig.2b-c and 3b. For the maximum test temperature of 950°C, the amount of twinning decreases radically and very few twins are observed. Observations of twinning in nickel-based super alloys have previously been reported for OP-TMF tests [5, 9-10, 11], in situ tensile tests [12] and creep tests [13-14] in the temperature interval 600°- 850°C. This indicates that the rate of deformation is not an important parameter for the formation of twins since several types of plastic deformation can cause twinning in the material. The twins are established by dislocations that are identical to Shockley partials a/6<112> and they move through the γ'-phase in closely-separated pairs on {111} planes [12, 14]. The motion of dislocations depends on the temperature and this determine if a twin will be formed or not in the superalloy. If a pair of Shockley partials a/6<112> glide in a viscous manner drawing long stacking faults behind them twins will be formed [12, 14]. However at higher temperature about 950°C the dislocation starts to climb [14-15] and the result is that no stacking faults are formed in the superalloy and consequently no twinning will occur.

In this study recrystallization has occurred in the grain boundaries and around particles for the test with a maximum temperature of 850° and 950°C. When the maximum temperature is 950°C, recrystallization has been more distinct and recrystallization has also occurred in the deformation structure see fig. 4a and 5a. Recrystallization at the grain boundaries and around particles has previously been observed and reported for other superalloys and during the recrystallization the γ'-phase is dissolved at the migrating grain boundary. The γ'-phase is then sporadically reprecipitated in the new grains. However, in these cases, the material was plastically deformed, and then annealed at temperatures in the range of about 1050°-1200°C [16-17]. The dissolution of the γ'-phase is strongly influenced of its coherency and the γ'-phase will lose the coherency when dislocation networks are formed around them. This will lead to a dissolution of the γ'-phase more continuously and uniformly and the dissolving process is more controlled by local diffusion [18]. Recrystallization often occurred at grain boundaries, around particles and in deformation structures since the material is heavily deformed around or in these sites and this will act as nucleation

site for the recrystallization [17]. Another effect of plastic deformation is that it will decrease the recrystallization temperature which can be one of the explanations why recrystallization is observed for temperature down to 850°C in this study, however, it should be considered that the recrystallization temperature for pure nickel is 600°C [24].

5. Summary

Most cracks have propagated transgranularly through the material and this holds for all temperatures used in this study. All cracks which are formed in the material have initiated and started to propagate in deformation structures such as deformation bands formed in the most plastically deformed areas of the material. In the temperature interval 750°-850°C, twins are formed in both IP and OP TMF-tests and this behaviour is observed to be further enhanced close to a crack. Twins are to a significantly lesser extent observed for tests with a higher (950°C) maximum temperature. Recrystallization has occurred at grain boundaries and around particles for tests with a maximum temperature in the interval 850°-950°C. For the temperature 950°C, recrystallization has also occurred within deformation bands.

Acknowledgements

The work was financially supported by Siemens Industrial Turbomachinery AB in Sweden, the Swedish Energy Agency via the Research Consortium of Materials Technology for Thermal Energy Processes under grant no: KME-502 and by the Swedish Research Council under grant no: 60628701.

References

[1] J.R. Davis (Ed.), ASM Speciality Handbook: Heat-Resistant Materials, ASM International, Materials Park OH, 1997.
[2] M.J. Donachie, S.J. Donachie. Superalloys: A Technical Guide, second ed., ASM International, Materials Park OH, 2002.
[3] R.C. Reed, The superalloys: fundamentals and applications, Cambridge University Press, Cambridge UK, 2006.
[4] D. Arrell, M. Hasselqvist, C. Sommer, J. Moverare, On TMF Damage, Degradation Effects, and the Associated T^{MIN} Influence on TMF Test Results in γ/γ' Alloys, in: Green KA, Pollock M, Harada H, Howson TE, Reed RC, Schirra JJ, Walston S (eds9, Superalloys 2004, The Minerals, Metals & Materials Society, Warrendale (PA), 2004, p.291.
[5] J.J. Moverare, S. Johansson, R.C. Reed, Acta Mater. 57 (2009) 2266-2276.
[6] Z.F. Zhang, Z.G. Wang, Z.M. Sun, Acta Mater. 49 (2001) 2875-2886.
[7] Y. Li, S.X. Li, G.Y. Li, Mater. Sci. Eng. A 372 (2004) 221-228.
[8] C. Buque, J. Bretschneider, A. Schwab, C. Holste, Mater. Sci. Eng. A 300 (2001) 254-262.
[9] J.X. Zhang, Y. Ro, H. Zhou, H. Harada, Scripta Mater. 54 (2006) 655-660.
[10] J.X. Zhang, H. Harada, Y. Ro, T. Koizumi, T. Kobayashi, Acta Mater. 56 (2008) 2975-2987.
[11] J.X. Zhang, H. Harada, Y. Koizumi, T. Kobayashi, Scripta Mater. 61 (2009) 1105-1108.
[12] M. Kolbe, Mater. Sci. Eng. A 319-321 (2001) 383-387.
[13] M. Legros, N. Clément, P. Caron, A. Coujou, Mater. Sci. Eng. A 337 (2002) 383.
[14] L. Kovarik, R.R. Unocic, J. Li, P. Sarosi, C. Shen, Y. Wang, M.J. Mills, Prog. Mater. Sci. 54 (2009) 839-873.
[15] F. Jiao, D. Bettge, W. Osterle, J. Ziebs, Acta Mater. 44 (1996) 3933-3942.
[16] A.J. Porter, B. Ralph, Mater. Sci. Eng. 59 (1983) 69-78.
[17] M. Dahlen, L. Winberg, Acta Metall. 28 (1980) 41-50.
[18] T. Grosdidier, A. Hazotte, A. Simon, Scripta Mater. 30 (1994) 1257-1262.
[19] D.R. Askland, P.P. Phulé, The Science and Engineering of Materials, fifth ed., Thomson, Toronto, 2006.